Transactions of the Materials Research Society of Japan 33[3] 529-534 (2008)

Application of GISAXS to the Microstructural Evaluation of Semiconductor and Metallic Materials

H.Okuda[1], K.Kuno[1], M.Ohtaka[1], S.Ochiai[1], K.Ito[2], S.Sasaki[3], M.Tabuchi[4] and Y. Takeda[4]

[1]International Innovation Center / Dept. Mater. Science and Engineering, Kyoto University, Sakyo-ku Kyoto 606-8501
Fax: 81-75-753-5193, e-mail: okuda@iic.kyoto-u.ac.jp
[2]Riken. Kohto, Sayo 679-5198
[3]JASRI/SPring8 Kohto, Sayo 679-5198
[4]VBL/Dept. Mater. Science, Nagoya University, Furo-cho, Nagoya 464-8601

GISAXS measurement activities on semiconductor nanodots and metallic clusters/nanodots at Photon Factory and SPring8 by us are presented. Semicondutor nanodots have been one of the most well known inorganic materials examined as a model sample for GISAXS. Comparing the GISAXS results from the second generation source and those from the third one, it is concluded that the second generation would be sufficient if the conventional beam size and the coherence are required. Size, shape and spatial arrangements of only single layer of encapsulated nanodots have been assessed by the GISAXS measurements at Photon Factory. The examples shown in the present manuscript suggest that conventional SAXS beamlines at second generation source have enough potential to explore time-resolved measurements on the evolution of nanostructures at surface. Some extensions concerning GISAXS measurements are discussed.

Key words: GISAXS, nanodots, precipitation, kinematical analysis, DWBA

1. INTRODUCTION

Small-angle X-ray scattering (SAXS) in grazing incidence condition, GISAXS, is getting more and more familiar as a tool to analyze microstructures of thin films and multilayers. For example, number of proposals concerning GISAXS is increasing rapidly in SAXS beamlines at synchrotron facilities, in particular, on polymer materials, are increasing rapidly. Developments on optical components such as mirrors and 2-dimensional detectors with high sensitivity also open a possibility of GISAXS at laboratory sources on commercial basis. Therefore, some of the GISAXS measurements that used to be specific applications of the strongest SR beamlines, such as size distribution analysis of heavy nanoparticles, have already become conventional measurements. Therefore, we need to examine what is the topics to be promoted on the beamlines. To discuss these points, it is helpful to survey the results obtained at bending magnet beamlines at Photon Factory (Tsukuba) and SPring8 (Hyogo). In the following sections, some examples from BL-15A of Photon Factory and BL40B2 of SPring8 concerning microstructure evaluation of inorganic materials, i.e., semiconducting nanodots and metallic nanodots are shown.

2. METHODS : GISAXS AT SPRING8 AND PHOTON FACTORY

2.1 Ex-situ measurements on semiconducting nanodots at Photon Factory

Shape, size, and spatial distribution of self-organized semiconductor nanodots have attracted attention as a candidate that tailor the materials properties though quantum size effects[1][2]. Comparing quantum well structures, quantum dots may suffer the effect of interdiffusion. It may become more serious when the nanodots are encapsulated. Concerning the nanodots at the surface, there has been a lot of reports with a use of scanning probe microscopy (SPM). These studies have proven that the size and size distribution may be controlled by choosing optimal growth conditions, such as those for growth temperatures, growth rate, and growth interruptions. However, the change occurring during and after the overgrowth is still an open question, although some cross-sectional transmission electron microscopy (X-TEM) works[3] have demonstrated that clear shape change occurs at higher temperature growth. An ex-situ GISAXS measurement is a non-destructive method ideal for static evaluation of embedded microstructures. As reported previously[4]-[7], use of small-angle scattering beamline and a two-dimensional detector + Imaging plate system is the most convenient solution for GISAXS measurements. Figure 1 is a schematic illustration of the measurements used for semiconducting and metallic nanodots at BL-15A of photon factory. The wave length is fixed at 0.15 nm. The beam was focused onto the detector plane at the size of about 0.2 mm [8]. For quantitative analysis, Imaging Plate was used to record the intensity. Since the nanodots on (001) substrates may have facetted structures depending on the size and the growth conditions, scattering patterns were recorded for several in-plane directions of incidence, including [110] and [100]. Ge nanodots encapsulated by Si and InAs nanodots encapsulated by amorphous As were examined in the present measurements.

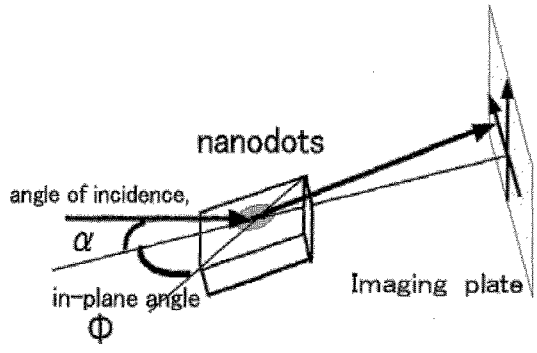

Fig. 1 GISAXS setup at BL-15A of Photon Factory for semiconducting nanodots. The angle of incidence is set to be larger enough than the critical angle.

2.2 In-situ measurements on formation processes of islands in thin metallic films

For time-resolved measurements, the only detector available at this moment for GISAXS with a frame rate more than a frame per minute is ccd with image intensifier (II-CCD). In the present measurements, we used II-CCD with 6 or 9 inch II. These detectors have excellent sensitivities to catch very weak GISAXS signals. The main drawback is small dynamic range of the detectors. Therefore, the detectors were mainly used to examine the low-q region, i.e., the interparticle interference and the Guinier region. This is enough when we are interested in the temporal evolution of the size and the shape, which are the central issues in the time-resolved measurements.

3. RESULTS

3.1 Ge nanodots capped with Si layers

Concerning morphological evolution of Ge nanodots grown on Si (001) by MBE, it has been demonstrated that the Ge nanodots should be facetted [9]-[10] by preceding works utilizing SPM and GISAXS for the nanodots at the surface. It is true for relatively large nanodots having a diameter of tens to hundreds of nanometers. From thermodynamical viewpoints, such nanodots, or sub-micron-dots should naturally have facets. However, the questions are that whether, 1. the as-grown nanoscale dots have facets in the early stage of 3 dimensional growth in SK mode, 2. as-embedded nanodots have facets, and 3. whether interdiffusion occurs during overgrowth of the nanodots.

Ex-situ GISAXS measurements with large dynamic range are suitable for such discussions. Figure 2 gives a GISAXS pattern of Ge nanodots grown by molecular beam epitaxy and then capped with a Si layer. The profile is shown for φ=0.0 degree, i.e., [110] incidence. The two-dimensional intensity profile has no clear streaks, meaning that nanodots do not have facets. Guinier plots and interparticle distances as a function of in-plane angle, shown in Fig. 3, suggest that the shape and the spatial distribution of the Ge nanodots embedded in the Si cap layer is isotropic. The present result is quite different from the preceding works by a German group [11], suggesting a strong spatial anisotropy and correlation due to elastic interactions.

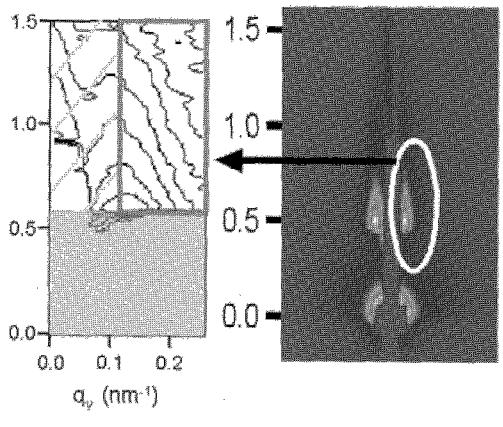

Fig. 2. GISAXS contour and the whole pattern obtained for Ge nanodots grown by MBE and capped with about 40 nm of Si layer.

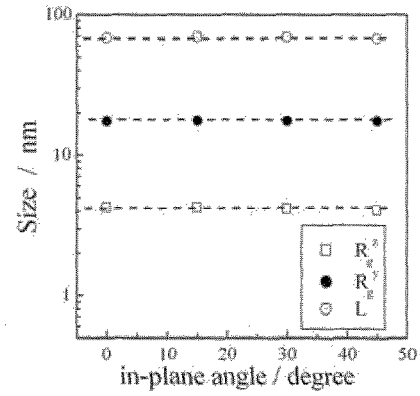

Fig. 3. Gyration radius in z and y directions, and the interparticle distance obtained from GISAXS pattern for Ge nanodots capped with Si layer. The in-plane angle corresponds to the angle between the in-plane direction of the incidence and [110] of the substrate.

The structure parameters deduced from Fig. 3, in contrast, suggest that the Ge nanodots are isotropic in shape and spatial arrangements. It is reasonable when one takes the fact that interfacial energy is the key factor that determines the nanostructure into account.

These results, although the size of the nanodots in concern is much smaller than the preceding works, suggests that static evaluation of nanodots with a size of several to ten nanometers requires bending magnet beamlines at second generation source, if the experimental condition is chosen appropriately. For example, single exposure at BL15A requires just 10 to 20 seconds for II-CCD, and about 5 to 10 minutes for Imaging Plate. In contrast, when we are interested in the

interface structure, the statistics required at the Porod's region is sometimes too long exposure time for small nanodots. Use of insertion devices becomes necessary for such cases. The use of Porod's law for GISAXS is, however, rather complicated for several reasons. One point is that form factor of the dots has lower symmetry than the shapes treated in transmission SAXS, since the dots are grown on a substrate and generally do not have symmetry in z (growth) direction. The other is the effect of reflected beam, i.e., correction due to DWBA calculations. In principle, the effect of form factor of the nanodots can be examined by fitting the whole 3-dimensional scattering intensity with a model shape. Isotropic in-plane shape observed in the present work simplified the procedure, since the shape of the nanodots can be expressed in one dimensional function. As reported previously [6], we introduced a model shape function as a rotation of $y=1-x^n$ around z axis. Fitting the two-dimensional intensity pattern with the model function gave a best fit with n=2, that is, rather a dome shape. The gyration radii obtained by the Guinier approximation of the in-plane and out-of-plane cuts of two dimensional intensities can be now translated into the real size of the nanodots. From n=2 and R_y=18 nm, R_z=4.2 nm, it is concluded that the average size of the nanodots are 40 nm in diameter, and 9 nm in height, with in-plane interparticle distance, L =70 nm.

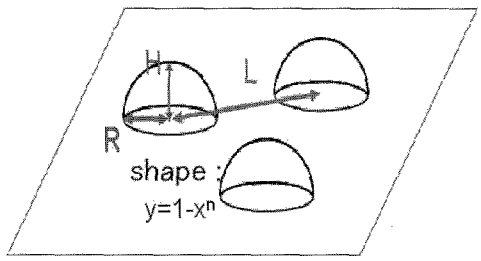

Fig. 4. Schematic illustration of the Ge nanodot structure obtained from the GISAXS. The nanodot layer is capped by a Si layer with about 40 nm in thickness.

As mentioned above, the separation of the two effects, an anisotropic shape effect and the core-shell structure effect requires a detailed analysis. In the experimental part, it is concluded that smaller Ge nanodots require a use of insertion devices to obtain reliable data at Porod's region. We are now working on both the intensity simulations and better experimental results on statistics and signal-to-noise ratio. We have observed a systematic deviation from the Porod's law at the intermediate q region, and quantitative analysis is now in progress. The other important point to be examined is the validity of Born Approximation (BA) in the shape analysis used in the fitting of the pattern. The main reason that BA is justified is that the angle of incidence, α in Fig.1 is 0.5 degree, much larger than the critical angle in the present measurements. Although the Si cap layer is smooth with the roughness of about 0.6 nm, common to such epitaxially grown materials, large angle of incidence gives low reflectivity that lead to very small correction to BA.

3.2 InAs nanodots on GaAs substrates

InAs has much larger difference in the lattice parameter against GaAs when compared with the combination of Ge and Si. Classical energy calculation predicts that for the overgrowth of such materials having as large misfits as 8 % with the substrate, the critical thickness of uniform layer growth is of the order of lattice parameter. It means that the onset of nanodot formation from pseudomorphic growth and subsequent relaxation may occur very easily. At the same time, the driving force for the stabilization of the structure by interdiffusion should be large. Therefore, the intermixing during the self-organization of nanodots and also that during epitaxial growth of a cap layer should be a much more serious problem for this alloy system. Therefore, it is quite important to know the morphological stability during the growth of the nanodots and cap layer. Concerning the nanostructures just after the growth of nanodot layer, it is not possible to examine the structure ex-situ, because the surface oxidizes very easily. Some preliminary examination also suggested that growth of epitaxial cap layer even at a low-temperature may alter the structure. Therefore, we prepared samples with amorphous As cap layers grown at room temperature after epitaxial growth of the InAs nanodots. The samples were quenched into room temperature by pulling out the sample from the growth chamber immediately after the growth of nanodots, and then a cap layer was evaporated onto the sample. The samples were kept in vacuum also during measurements.

Figure 5 shows a two-dimensional GISAXS pattern for the InAs sample grown at 653 K for 2 monolayers (ML) and then amorphous As layer at room temprature for 10 nm.

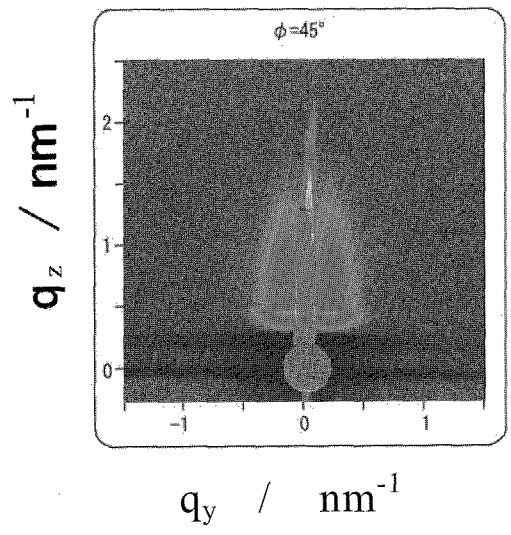

Fig. 5. Two-dimensional GISAXS profile for InAs layer grown on (001) GaAs substrate for 2ML and then capped with 10 nm of amorphous As layer. The in-plane direction of incidence is [100]. The circle at origin is the direct beamstop for transmission. No clear streaks are seen in the figure.

The in-plane angle of incidence is parallel to [100] and the q_z direction corresponds to [001]. The profile shows

a strong similarity with the pattern for Ge nanodots as shown in Fig. 2, and also with those in ref.[4]-[6], suggesting densely distributed dome-shaped nanodots. Preceding works [13],[14] suggest that faceting starts between the average layer thickness of 2 ML and 4 ML. Generally, the transition from unfaceted shape into facet structure is gradual. Therefore, we might expect a well-defined facet patterns for large nanodots and observe something in between for the intermediate layer thickness. The gyration radii for the nanodots grown for 2 ML are 4 nm and 1.5 nm in in-plane and out-of-plane directions respectively. This result suggests that the shape of the nanodots is flat for Ge nanodots. Clear interparticle interference is observed for 2 ML sample. The number density estimated from the peak is about $1x10^{11}$ /cm^2.

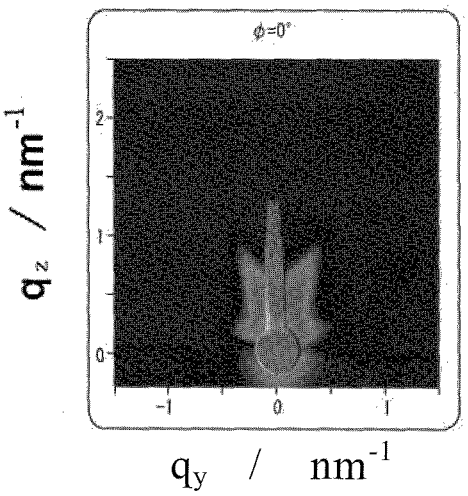

Fig. 6. Two-dimensional GISAXS profile for InAs layer grown on (001) GaAs substrate for 10 ML and then capped with 10 nm of amorphous As layer. The in-plane direction of incidence is [110].

Figure 6 shows a GISAXS pattern of InAs nanodots grown for 10 ML. It is clearly seen that the shape of the two-dimensional intensity pattern is not an isotropic dome, but a well-defined streak extending towards [113] and [-1 -1 3], meaning that the shape of the nanodots is now a well-defined facets composed of {113} planes.

Since the nanodot layer and the cap are composed of relatively heavy elements, with stronger contrast in the electron density, the scattering intensity for InAs samples were found to be stronger than that for Ge nanodots. Usually, it implies that the specular reflection is stronger for such samples, and the corrections from DWBA become important. However, the InAs nanodot samples examined here are found not to be treated by such approximations. As pointed out by the early work by Sinha et al,[15] modification of scattering intensity by DWBA holds when the perturbation is small enough compared with the main unperturbed wavefield. However, some results obtained for present samples rather indicate that BA should be used for the analysis.

First, the specular reflectivity obtained for the present sample, 4 ML InAs nanodots capped with a 10 nm of amorphous As layer, decreases quite rapidly with the angle as shown in Fig. 7. It is typical for rough surface. At the large angle with very weak intensity, for example, we could not observe even a well-defined specular

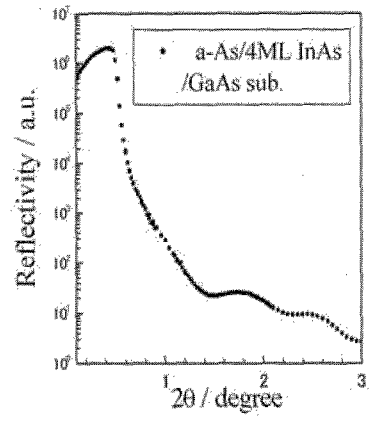

Fig. 7. Reflectivity of the a-As/InAs/GaAs samples obtained at an undulator beamline near the Ga K absorption edge. A rapid decay of the reflectivity is clearly observed, corresponding to large roughness at the amorphous As cap layer.

peak in the transverse scan of the sample at 2θ=2.0 degree, namely, the intensity at the specular point is mainly attributed to the diffuse scattering. Such rapid decay in specular reflectivity and strong diffuse scattering make the specular spot at in the GISAXS pattern invisible. GISAXS patterns shown in Figs. 5 and 6 indicate another feature that dynamical effect is not strong in these samples. As shown by Lazzari et al[14], the streaks originated from facets and Yoneda line split when the effect of reflected beam is strong. This effect is observed in particular clearly when the nanodots have facetted structure, since the dynamical effect simply shifts the streaks that run in diagonal direction in q_z direction, thereby two parallel streaks being observed. Figure 6 has only one set of streaks running in [113] and [-1 -1 3] directions. Therefore, the GISAXS pattern in Fig 6 shows no clear effect of reflected beam except that there is a slight enhancement of the intensity just around the Yoneda line, although the sample surface is a mirror surface and the average thickness of the layers grown on the GaAs substrate is quite thin.

As shown above, many microstructures with well-defined nanodots have internal structures that should be rather treated by BA, than DWBA. In general, a combination of GISAXS and reflectivity is attractive because the analysis of reflectivity is expected to give information on the wavefield of the layer that is a basis of DWBA correction in the GISAXS measurements. However, present results rather suggest that in many applications, the situation is not suitable for the assumption of small perturbation. Present analysis has been made within BA by avoiding the area close to Yoneda lines, and also chosing the angle of incidence so that the reflectivity is small.

3.3 Metallic nanodots

Another important application of GISAXS in the

inorganic materials is magnetic nanodots.
Since metallic nanodots are strong scatterers, the perturbation is too strong to be treated by DWBA once well-defined nanodots with high number density have developed. As reported previously, the initial state of such metallic nanodots is sometimes a uniform and smooth film which gives very strong reflections. Therefore, during the in-situ measurements of the formation process of nanodots, the observed GISAXS patterns are expected to be in a complicated situation that they shift from DWBA regime to the situation that may be better described by BA approximations. Validity of analysis for such microstructure change is still an open question, and detailed discussions by using model structures are under way by several researchers.

4. DISCUSSIONS

4.1 Use of second generation sources for GISAXS.

For static measurements, the stability and the signal-to-noise ratio, or the back ground level is the most important factor for GISAXS measurements. As shown in the preceding sections, a SAXS beamline at the second generation SR, i.e., beamline 15A of Photon Factory is sufficient for many of the GISAXS applications for thin nanostructure evaluations, such as the structure of nanodots mentioned above. For example, the exposure required to obtain single shot by II-CCD is about 15 to 30 seconds for these nanodots. It means that time resolved GISAXS measurements in conventional beamsize are suitable subjects for the beamline. On the other hand, when the sample is small, or the incident angle needs to be very low, i.e., below the critical angle. the beamsize, focusing optics in the SAXS beamline is not appropriate anymore. The SAXS beamline at PF uses a two dimensional focusing, with its focal point at the detector plane. It means that the beam size at the sample is rather large, and impossible to cut into a small beam without loosing most of the flux. Therefore, GISAXS under very small angle of incidence, e.g., 0.05 degree, for light thin films and for microbeam application, use of the third generation is essential. These applications are now under developments in the undulator beamlines at SPring8.

4.2 Use of anomalous dispersion

When samples contain several elements, and may have interdiffusion or partitioning, SAXS with anomalous dispersion is sometimes a powerful solution to analyze the heterogeneous nanostructures such as segregations, partitioning, and interdiffusion in the granular materials. Use of anomalous effect simply requires energy resolution of incident photon, with a moderate resolution that is often used for XAFS with conventional resolution.
From this viewpoint, GISAXS with a use of anomalous dispersion is a subject suitable for the materials research in the second generation synchrotron radiation source. However, there is no SAXS beamline available at PF for GISAXS which provides energy resolution required for anomalous scattering. Small-angle scattering with a use of anomalous dispersion, Anomalous SAXS (ASAXS) has been under development at SAXS beamlines in SPring8 now. Figure 8 is an example of the change of the real part of atomic scattering factors for Zr-based quaternary bulk metallic glasses at the K absorption edge of Zr. Although the sample has been examined by transmission ASAXS, it gives an idea how Anomalous GISAXS should work.

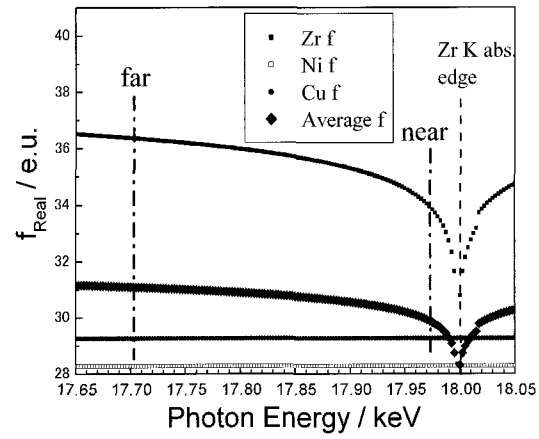

Fig. 8. Change of atomic scattering factors of ZrCuNiAl quaternary alloys at the K absorption edge of Zr.

In the transmission ASAXS, the SAXS intensity is simply given by the Fourier transform of the density distribution of atomic scattering factors. Therefore, the intensity is given as a function of incident energy as;

$$I(q,E_j)=\sum_{i,j} f_i(E_j)f_j(E_j)S_{ij}(q) \qquad (1)$$

with $f_i(E_j)$ the atomic scattering factor of i-th element at the incident photon energy of E_j. Therefore, the concentration distribution of each element can be assessed if the scattering intensities, $I(E_j)$ are measured precisely enough to be decomposed into partial structure. Or, when the number of energies is not enough against the number of unknown partial structure factors, $S_{ij}(q)$, then we may use two-phase analysis by assuming some microstructures[17]. In other words, if we intend to use the anomalous dispersion effect in full, it is quite important that the SAXS intensities should be normalized precisely enough between different photon energies. When we work on GISAXS, this point is quite important because stability of the beam position, size and sample height may also affect the normalization process through the change in the footprint effect. As reported by Rauscher et al.[18], GISAXS intensity for nanodots may be expressed for exposed dot structure as ;

$$A(q,ki,kf)=-k_0^2(1-n^2)\frac{e^{ik_0r}}{4\pi r}\{\Phi(q_{//},q_z) + R^f\Phi(q_{//},-k_z^f-k_z^i)+R^i\Phi(q_{//},k_z^f+k_z^i) + R^iR^f\Phi(q_{//},-q_z)\} \qquad (2)$$

where the form factor itself is identical as that appears in the transmission ASAXS. A closer look at (2) implies that anomalous reflectivity measurement is also desirable to analyze the correction term, where the anomalous effect of the wetting layer of the nanodots, which does not give SAXS intensity but changes the

reflectivity, is important for quantitative assessment of intensity.

This conclusion again recall the requirements on normal GISAXS that, combined reflectivity and GISAXS measurements are useful in DWBA analysis of GISAXS analysis, and at the same time, DWBA is sometimes not suitable in the actual nanodot structures as we have already shown. Owing to the difficulty mentioned above, fully quantitative AGISAXS is not successful although many attempts have been under way in SPring8 and also several other SR facilities.

References

[1] Semiconductor Quantum Dots, ed. Y. Masumoto and T.Tagahara, Springer Verlag, Berlin 2002.
[2] V.Ustinov, A.Zhukov, A. Egorov, N. Maleev, Quantum Dot Lasers, Oxford UP N.Y. 2003.
[3] O. G.Schmidt, U. Denker, K. Eberl, O. Kienzle and F. Ernst Appl. Phys. Letters, 77(2000) 2509-2511.
[4] H. Okuda et al., Appl. Phys. Lett. 81(2002)2358-2360.
[5] H. Okuda and S. Ochiai, J. Mater. Res. Soc. Jpn 28 (2003) 27-30.
[6] T. Ogawa, H. Niwa, H. Okuda and S. Ochiai Mater. Science Forum, 475-479(2005)1097-1100.
[7] H. Okuda, M. Ohtaka, Y. Sakai, K. Kuno, S. Ochiai, T. Ichitsubo, E. Matsubara, S.Sasaki and K. Inoue Proc. Workshop on Buried Interface Science with X-rays and Neutrons, KEK proc. 2006-3(2006) 117-122.
[8] Y. Amemiya, K. Wakabayashi, T. Hamanaka, T. Wakabayasi and H. Hashizume. Nucl. Instrum. Method, 208 (1983) 471-476.
[9] A. Chaparro, Y. Zhang, J. Drucker, D. Chandrasekhar and D. Smith, J.Appl. Phys. 87(2000) 2245-2254.
[10] A. Rastelli and H. Kanel Surf. Sci. 515 (2002) L493-498.
[11] I. Kegel, T. Metzger, J. Peisl, P. Schittenhelm and G. Abstreiter Appl. Phys. Lett., 74(1999)2978-2980.
[12] Y. Nabetani, T. Ishikawa, S. Noda, J.Appl.Phys. 76(1994),347-351.
[13] K.Jacobi Prog. in Surf. Sci. 71 (2003),185-215.
[14]S.K.Sinha , E.B.Sirota, S.Garoff and H.B. Stanley, Phys. Rev. B 38(1988) 2297-2311.
[15] R.Lazzari, J.Appl.Cryst.,35(2002)406-420.
[16] H.Okuda, S. Ochiai, M. Ohtaka, T. Ichitubo, E. Matsubara, N. Usami, K. Nakajima, S. Sasaki and O. Sakata Trans. Mater. Res. Soc. Japan, 32(2007)275-280.
[17] O.Lyon and J.P.Simon, Acta Metall., 34(1986), 1197-1202.
[18] M. Rauscher,T.Salditt and H. Spohn, Phys. Rev. B52 (1995) 16855-16863.

(Recieved December 10, 2007 ; Accepted April 25, 2008)